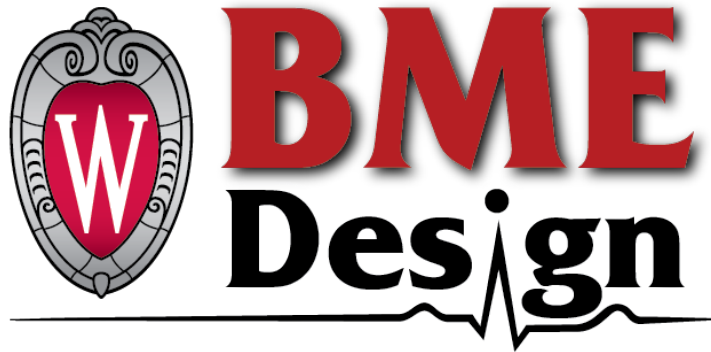


Optical Imaging of the Small Airway Mucosa

Biomedical Engineering Design 200/300



Department of Biomedical Engineering
University of Wisconsin-Madison
December 14, 2022

Team Members:

Peter Wawrzyn (Team Leader)
Jade Berget (Communicator)
Andy Slayton (Co-BSAC)
Lily Zahn (BWIG)
Yash Shah (Co-BSAC)
Sofia Castagnozzi (BPAG)

Client:

Dr. Allan Brasier MD
UW Institute for Clinical and Translational Research, Executive Director

Advisor:

Dr. Filiz Yesilkoy PhD
UW Madison College of Engineering - BME

Abstract

Airway diseases are an increasingly common issue in many humans and the need for effective treatments has never been greater. In order to effectively test these treatments, accurate imaging of the airway mucosa is required. In humans this has been done effectively using Optical Coherence Tomography (OCT) imaging; however, using OCT in mouse test subjects for visualization of the airway mucosa has yet to be demonstrated. The goal of this project is to create an imaging method for the airway mucosa of a mouse test subject in vivo. Specifically, this semester the goal is to create a mechanism that can fully rotate and retract an optical fiber in an airway catheter. The device was designed in a modular fashion so the mechanics of retracting and rotating the fiber occur outside the subject. This includes two motors, one motor with the function of retracting the optical fiber, and one motor with the function of radially spinning the optical fiber. This design uses a clear catheter shell to allow for access and then imaging of the airway mucosa. The prototype includes a base with an axle and two bearings, two servo motors, a circuit board, and an optical fiber. Testing was done to evaluate three different criteria: retraction consistency, 360° rotation, and 90° light deflection. Future work for the project includes properly scaling the overall design to work effectively using a mouse subject.

Abstract	1
I. Introduction	4
II. Background	4
Client Information and Preliminary Research:	4
Design Specifications:	5
III. Preliminary Designs	5
1. Clear Intubation Catheter:	5
2. Helical Balloon Catheter:	6
3. Flexi-Catheter Withdrawal Design:	7
IV. Preliminary Design Evaluation	8
Material Evaluation	10
Proposed Final Design - Probe and Spinning Mechanism	11
V. Fabrication/Development Process	14
Materials	14
Methods	15
Final Prototype	15
Testing	17
VI. Results	17
VII. Discussion	18
VIII. Conclusions	19
IX. References	20
X. Appendix	22
A: Product Design Specification	22
B: Testing Data	27
C: Team Expenses	28
D. Computer Aided Design Models (all dimensions in inches)	29
E. Fabrication Protocol	30
F. Arduino Code	31

I. Introduction

Common airway diseases include asthma, chronic obstructive pulmonary disease (COPD), pulmonary fibrosis, pneumonia, bronchiectasis and lung cancer. These are diseases that most people have been affected by, whether themselves or someone they know. Each of these diseases can affect any gender, race, or age and have varying harmful effects. Asthma affects about 14% of children 5 and under and COPD accounts for about 55% of respiratory diseases in both men and women. In 2017 there were 3,914,196 deaths due to chronic respiratory diseases which accounted for 7% of total deaths globally. This put chronic respiratory diseases as the third leading cause of death in 2017, just behind cardiovascular diseases and neoplasms. These rates have only increased since 1990 [1] and the only way to combat this issue is by developing treatments.

The cells lining the airway play an important role in common airway diseases. The mucosa will change thickness as the body's reaction to certain diseases or infections. When the mucosal lining in the airway thickens it restricts airflow and breathing becomes more difficult [2]. Part of testing treatment effectiveness is to measure that change in thickness of the mucosa.

New therapeutics are being developed for treatment, but a limitation in the work to develop these therapeutics is the difficulty of measuring changes over the course of an experiment in small animal studies. An imaging technique being used now is Optical Frequency Domain Imaging (OFDI), a second generation approach of Optical Coherence Tomography (OCT). OFDI is able to monitor changes in the airway; however, the current probes used with this imaging modality are too large for small animal testing. B. J. Vakoc et.al. developed and used a balloon stabilization device for OFDI imaging in the distal esophagus of swine [3]. However, a similar approach within a mouse airway would exert excess pressure on the trachea, potentially harming the mouse. L. P. Hariri et. al developed a custom bronchoscope for use of OFDI imaging in human lungs, however, the device is too large to use in mice and difficult to scale [4]. Due to this problem, the goal of this project is to create and validate an miniaturized OFDI, or broadly classified OCT, probe for imaging in the airway of small animals; specifically, creating an imaging probe to be utilized on mice. The project has a potential global impact of setting up the foundation for small scaled imaging and drug testing on animals. The final design is also environmentally friendly as it is intended for reusability with sterilization. Through this project, scientists like Dr. Brasier can help research diseases like asthma and further society in the development of new drugs to alleviate asthma or other airway related disease symptoms.

II. Background

Client Information and Preliminary Research:

Dr. Brasier is researching treatments for inflamed and diseased airways. In their research, the lab is testing the effectiveness of treatments on the airways of small animals. The airway mucosa, which consists of epithelial cells lining the esophagus, varies in thickness between

healthy and diseased airways. Monitoring the thickness of the airway mucosa can indicate the effectiveness of treatments for lung diseases [5]. Dr. Brasier is looking to monitor changes in the thickness of the mucosa of mice while testing the effectiveness of their lung disease treatment. One method of measuring the mucosa thickness is to use optical imaging, specifically OFDI with a probe device.

Optical frequency domain imaging, or OFDI, uses infrared light to generate cross-sectional images of tissue with a resolution between 10 and 20 micrometers [6]. The theory behind OFDI imaging is to direct light waves at tissue and measure the delays of the back-reflected light to estimate the thickness of the tissue [6]. To produce accurate imaging, the device must be stable and able to collect and transmit data to an external imaging device.

Design Specifications:

The goal of this overall project is to create a probe capable of performing OFDI imaging on the small airway mucosa of mice. The device must be small enough to fit within the mouse airway, which is approximately 1.5 mm in diameter. [7] The device must be kept stable enough to use OFDI to create a 3D map of the airway, measuring the depth of the airway mucosa up to 1 mm and resolution between 5 and 20 micrometers [6] with a Signal to Noise Ratio of at least 80 [8]. The device will be used several times on living mice over several weeks, so it must be reusable with up to code biocompatible materials and meet the clients lab animal testing policies along with federal regulations [9]. The project has a budget up to \$10,000, but that can vary depending on the availability of optical imaging equipment.

For this semester, the team focused on the development of the spinning mechanism for the probe. The spinning mechanism must allow for translational and rotational motion, with both being easily adjustable. The mechanism must provide reliable 360 degree rotation of the optical fiber within the mouse airway, and must reliably retract the optical fiber from the mouse airway.

III. Preliminary Designs

1. Clear Intubation Catheter:

The clear intubation catheter design contains a clear outer catheter that is designed to hold the mouse airway in place during imaging. The imaging probe, that will be connected to an optical fiber, will be inserted inside this clear catheter. The outer clear catheter will ensure that the airway is not only stable, but also keep the airway safe from potential damage. Figure 1 shows an imaging probe being inserted into a clear catheter which will be in the airway. The diameter of this catheter will be 1.2mm and the length of the catheter will be 15mm to precisely fit into the airway of a mouse.

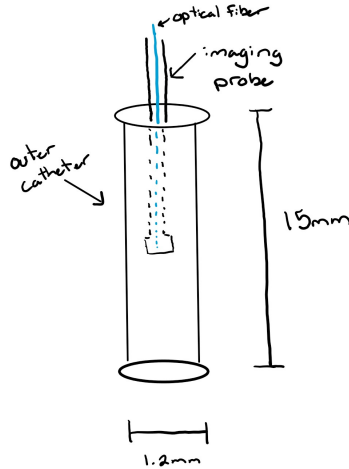


Figure 1: Clear intubation catheter with probe insertion.

2. Helical Balloon Catheter:

The helical balloon catheter design contains a small deflated balloon covering on the outside of a helical shaped catheter during insertion. Once the helical catheter has been inserted into the mucosa, the balloon is then inflated in order to stabilize the airway for accurate and safe imaging. The balloon would only cover the body of the catheter, leaving the tip exposed for the imaging probe. With nothing covering the imaging probe, there will be higher resolution with no extra artifacts. The dimensions of this catheter with an inflated balloon would be 1.0mm in diameter and 5.0mm in length. Figure 2 shows an image of the overall design of the catheter during insertion, where the balloon surrounds the body of the catheter waiting to be inflated for imaging. Figure 3 shows how the catheter will look during imaging with the balloon inflated to stabilize the airway.

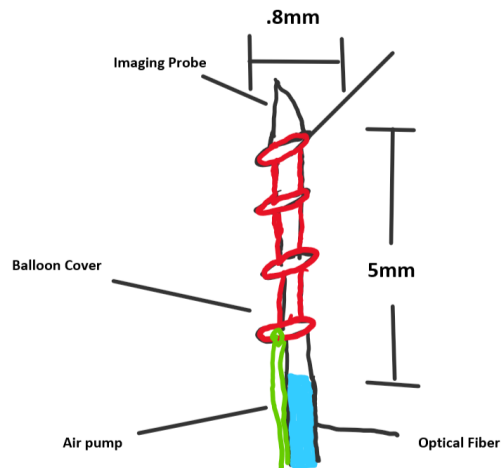


Figure 2: Helical Balloon Catheter with balloon deflated for insertion.

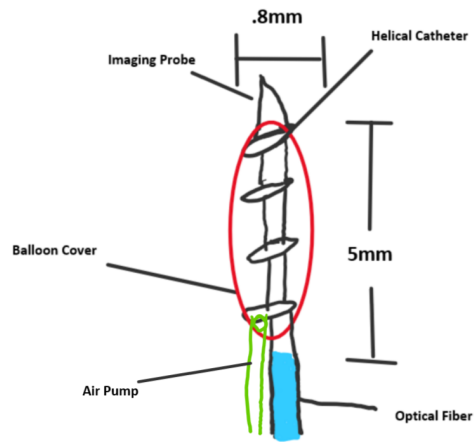


Figure 3: Helical Balloon Catheter with balloon inflated (colored red) for stabilization during imaging.

3. Flexi-Catheter Withdrawal Design:

The Flexi-Catheter Withdrawal design consists of an outer catheter and an imaging probe. The outer catheter acts as a normal catheter but contains the imaging probe housed inside of it. The outer catheter is used as a mechanism to guide the imaging probe into the mouse airway. The outer catheter is then retracted exposing the imaging probe which allows for imaging of the mouse airway mucosa. Figure 4 shows an image of the probe mechanism at the time of imaging. In Figure 4 the outer catheter is retracted exposing the imaging probe to the airway mucosa for imaging.

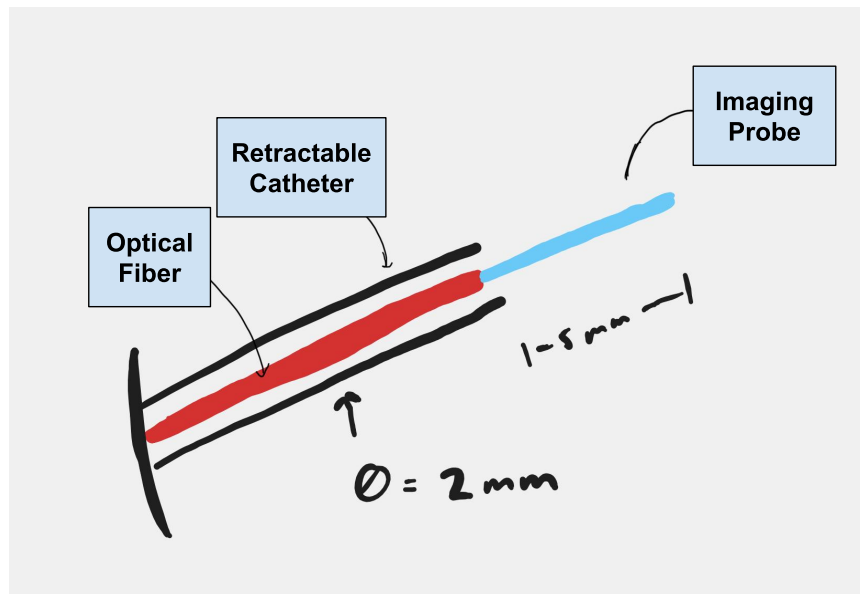


Figure 4: Flexi-Catheter Withdrawal Design with the outer catheter in the retracted position.

Figure 5 shows the probe mechanism with the outer catheter advanced forward. This configuration would be used when the probe is being navigated into and out of the mouse airway.

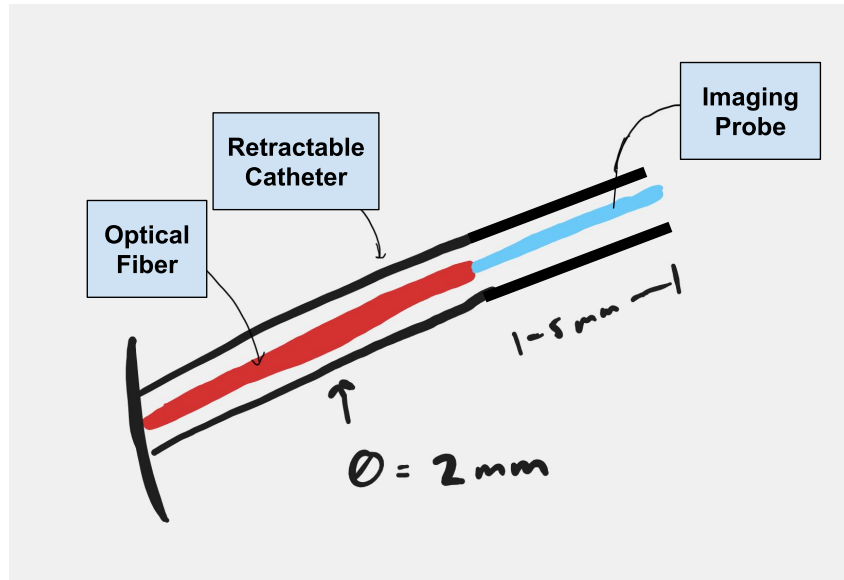


Figure 5: Flexi-Catheter Withdrawal Design with the outer catheter in the advanced position

IV. Preliminary Design Evaluation

In order to evaluate the three different designs, a design matrix shown in Table 1 was created. All three designs were judged based on their anticipated Stability (30), Manufacturability (25), Accuracy (25), Safety (15), and Cost (5).

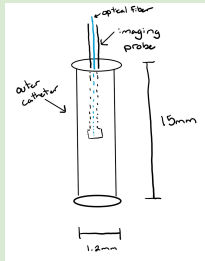
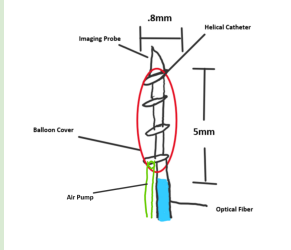
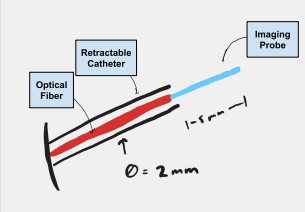
The stability of the probe and airway was the highest weighted category at 30 because keeping the airway open and stable while imaging is a key for accurate imaging. The Clear Intubation Catheter scored 5/5 because with the outer catheter in place the airway will be completely open during the entire imaging process with the probe free to move and rotate inside. The Helical Balloon Catheter scored 4/5 because the entire airway does not stay open during imaging but the balloon can add stability around the tip of the probe. The Flexi-Catheter Withdrawal Design scored the lowest at 2/5 because there is no outer component that guarantees the airway to stay open around the probe.

Manufacturability of the probe mechanism was tied for the second highest weighted criteria. This category measured the ease at which the probe mechanism could be manufactured. The Clear Intubation Catheter scored the highest with a 5/5 due to the simplicity of the design. The Flexi-Catheter Withdrawal Design scored second highest with a 4/5 due to the potential difficulty manufacturing the mechanism needed to withdraw the outer catheter. The lowest scoring design was the Helical Balloon Catheter with a score of 3/5 due to the complex nature of

manufacturing a balloon small enough for a mouse airway and incorporating that into a helical catheter.

Table 1: The Design Matrix used to rank the preliminary designs across five weighted criteria. Green highlights are the winner of that section

Probe Mechanism

Design Criteria	Clear Intubation Catheter		Helical Balloon Catheter		Flexi-Catheter Withdrawal Design	
						
Stability (30)	5/5	30	4/5	24	2/5	12
Manufacturability (25)	5/5	25	3/5	15	4/5	20
Accuracy (25)	3/5	15	5/5	25	5/5	25
Safety (15)	5/5	15	1/5	3	3/5	12
Cost (5)	5/5	5	4/5	4	5/5	5
Total (100)	90		71		74	

The accuracy that the probe mechanism allows for was tied for the second highest weighted criteria at 25. This category intended to measure the accuracy and resolution that the probe design would allow for an OCT scanning system. The Flexi-Catheter Withdrawal Design and Helical Balloon Catheter both scored a 5/5 for this category because they both allowed for unobstructed visualization of the airway mucosa during imaging. The Clear Intubation Catheter scored a 4/5 on this category because it would require imaging through a clear catheter which could lead to artifacts in imaging and would lead to increased complexity in obtaining accurate imaging.

Safety of the probe was weighted at 15 due to the use with live mouse subjects. This category intended to judge how safely the device could be inserted into a mouse airway. During in vivo imaging of a mouse subject it is important to not damage the airway for proper testing of airway mucosa medications. During the rating of designs the possibility of potentially harmful

parts and materials was considered. The Clear Intubation Catheter scored 5/5 due to the lack of complicated parts that could lead to injury. The Flexi-Catheter Withdrawal Design scored 3/5 due to the possibility of injury during the outer catheter withdrawal. The Helical Balloon Catheter scored a 1/5 due to potential for injury from inflating a high pressure balloon in the airway.

Cost was the lowest weighted criteria at 5 due to the high budget for the project. Additionally, the probe mechanism is a small portion of the project cost compared to the imaging component. Due to this all designs scored highly with, the Clear Intubation Catheter and the Flexi-Catheter Withdrawal Design both scoring 5/5 and the Helical Balloon Catheter scoring 4/5, due to added expense of the balloon mechanism.

The Clear Intubation Catheter scored the highest with 90 total points. This was largely due to the simplicity of the design which leads to easier manufacturability and increased stability compared to other designs.

Material Evaluation

For the intended creation of the imaging probe, the team examined choices for what outer material that would encase the OFDI technology. To evaluate possible materials, a design matrix shown in Table 2 was created. All three materials were ranked based on their anticipated Moldability and Manufacturability (30), Reusability (25), Safety (20), Shelf Life (15) and Cost (10).

Table 2: The Design Matrix used to rank the probe materials across five weighted criteria. Green highlights are the winner of that section

Probe Material						
Design Criteria	Polycarbonate		Polypropylene Copolymer (PPCO)		Silicone Rubber	
Moldability & Manufacturability (30)	4/5	24	2/5	12	5/5	30
Reusability (25)	5/5	25	4/5	20	5/5	25
Safety (20)	5/5	20	5/5	20	5/5	20
Shelf Life (15)	4/5	12	5/5	15	5/5	15
Cost (10)	5/5	10	2/5	4	4/5	8
Total (100)	91		71		98	

To fabricate the probe, the team will use the silicone rubber as the outer material for the imaging technology as it ranked the highest in total for the criteria, and has many properties that make it favorable for biomedical applications. It is a firm and flexible material that can withstand a wide range of temperatures, chemicals, and UV exposure, making it ideal for sterilization conditions. It is also readily available, easy to manufacture inert, nontoxic, and nonbiodegradable, making it a suitable option for in vivo biotechnology. [10]

Proposed Final Design - Probe and Spinning Mechanism

The proposed final design consists of a clear intubation catheter made of silicone rubber encasing an optical fiber that directs light perpendicularly into the mouse airway, and a mechanism that both spins and retracts the catheter during imaging. The mechanism designed to support the original clear catheter design proposed during the preliminary presentations.

The clear intubation catheter will be able to be inserted into the mouse trachea. It will contain an optical fiber and with an angled mirror at the end that refracts light perpendicularly into the mouse airway. The mirror will attach to the end of the optical fiber such that both the mirror and optical fiber will rotate.

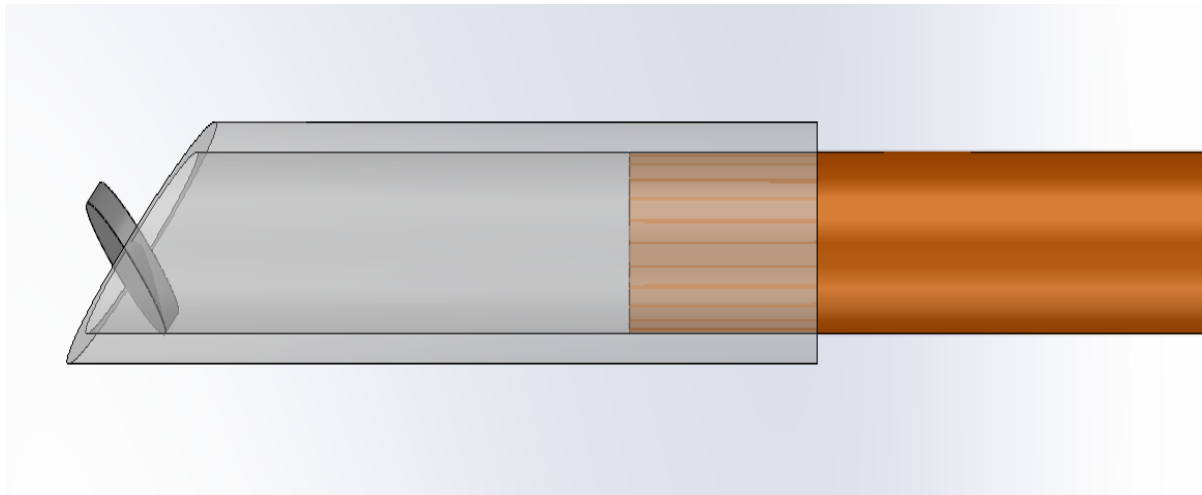


Figure 6: This shows a close-up view of the end of the catheter containing the optical fiber. This end will be inserted into the mouse trachea. The catheter allows the optical fiber to spin without injuring the mouse airway. The mirror allows for light to be refracted 90 degrees into the mouse airway.

The spinning mechanism will consist primarily of a base, a moving platform, and two servos. A belt drive with a servo will be used to spin an axle, which will be connected to a moving platform with high-tension string. When the axle spins, the platform will be able to move forward and back. The platform will sit above the axle and will be held in place with two guard rails. Another servo will sit on the moving platform and will allow for the spinning of the optical fiber. The servo will be connected to a 3D-printed piece that will hold the optical fiber. When the

servo spins, the connector will spin the optical fiber. The device will rotate from +180 to -180 degrees, allowing for a full 360 degree scan of the mouse airway.

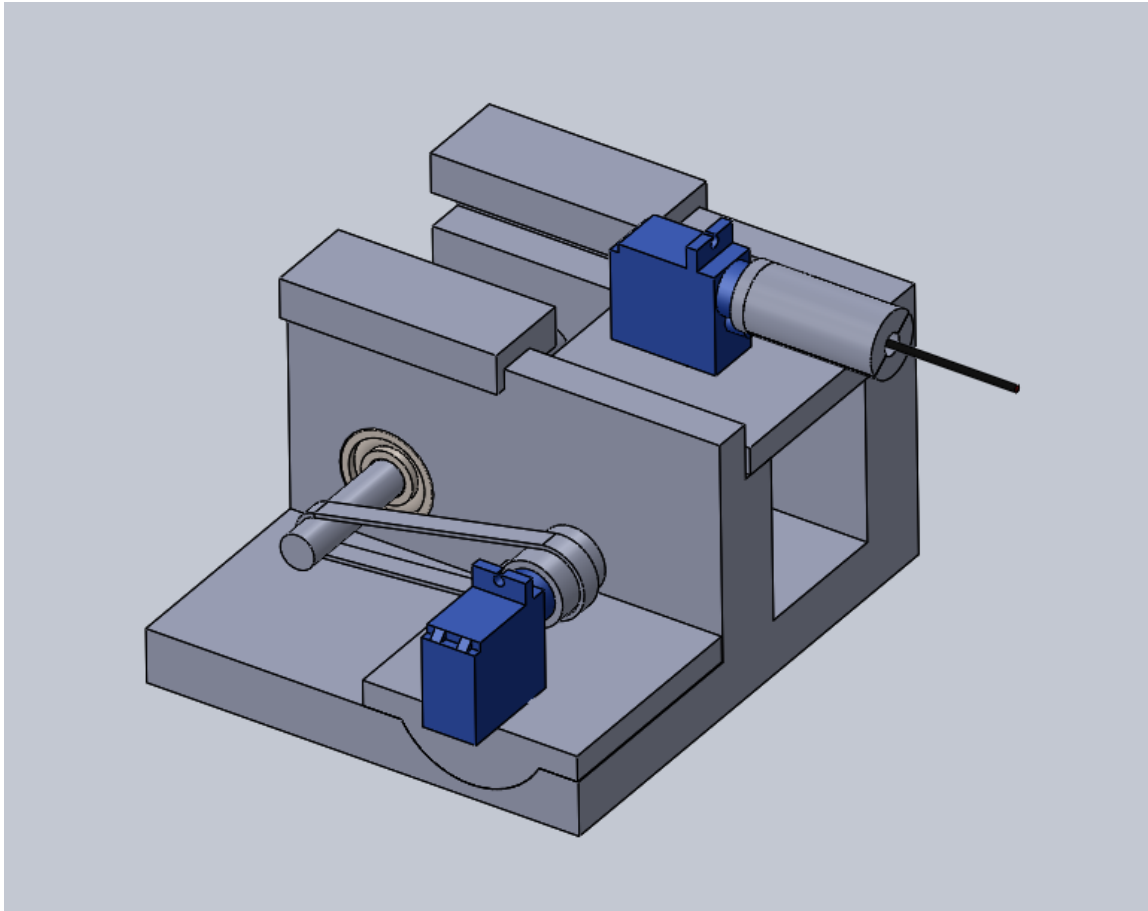


Figure 6: Front view of spinning mechanism in proposed final design.

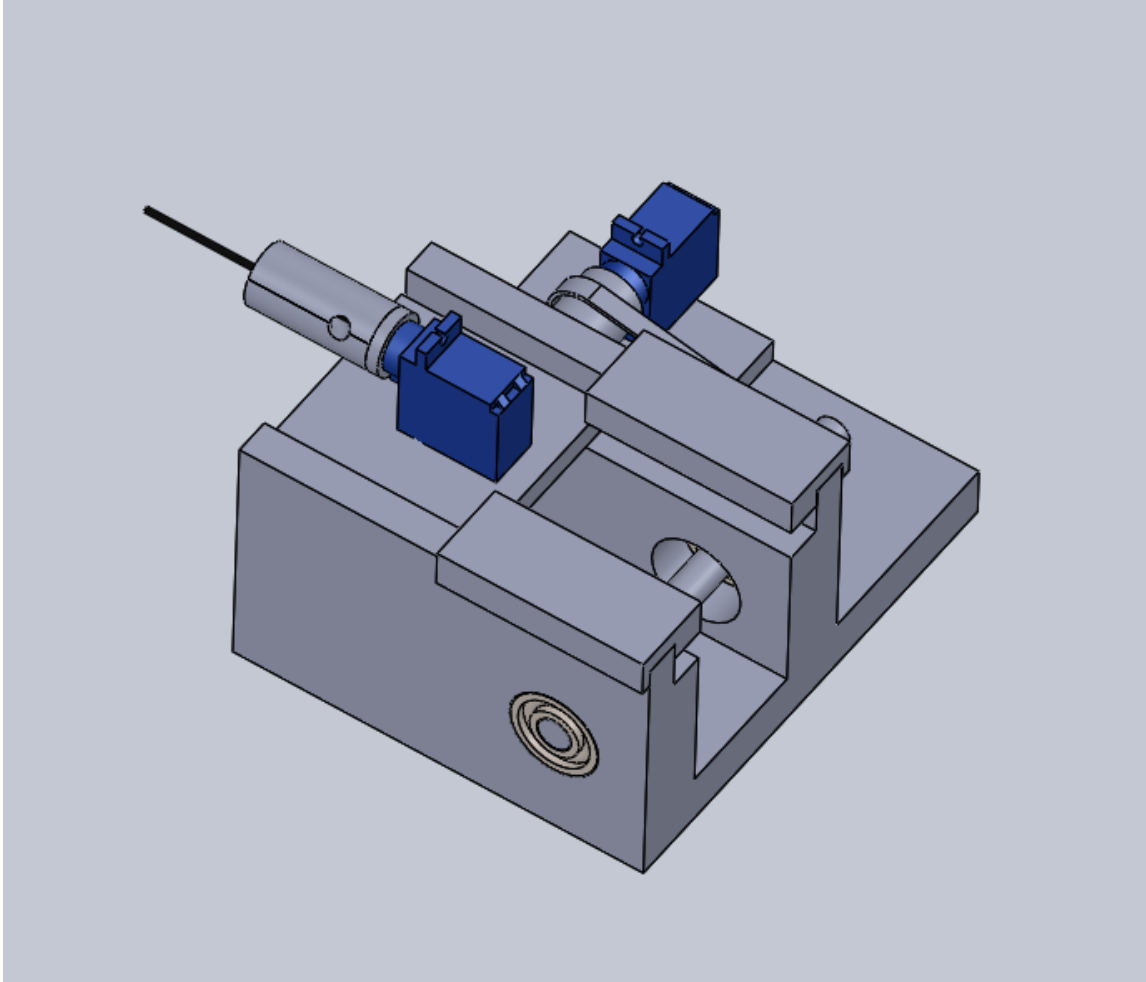


Figure 7: Back view of spinning mechanism in proposed final design.

V. Fabrication/Development Process

Materials

- A. Multimode optical fiber
- B. 8mm diameter catheter
- C. 2 360° 5V servo motors
- D. Arduino Uno microcontroller
- E. PLA plastic 3D-printed housing and platform
- F. 2 8x22x7mm bearings
- G. 1/4" wooden axle
- H. Rubber band
- I. 2 metal eyelets

Methods

The design for the spinning mechanism was modeled entirely in CAD software before fabrication. When a final design was decided, the base and platform were 3D-printed in PLA plastic. Features like inserts and holes were included in the print file, these allowed the servo motors and bearings to attach; this allowed for a faster fabrication process by ensuring correct dimensions without additional measurements. The axle was pre-cut to be incorporated into the mechanism. The retractable platform was attached at either side to a string which wrapped tightly around the axle. See Appendix E for a detailed fabrication process.

The circuit used to drive the components of the spinning mechanism was very simple. The servo motors received power from the arduino and were controlled digitally. The arduino microcontroller would receive an input signal associated with the push of a button. When this input was detected, the spinning servo motor was coded to spin 360° clockwise, then counterclockwise 360° to return to the initial position. While one servo motor is spinning, the other one is instructed to spin the axle, retracting the platform. See Appendix F for detailed code used for the Arduino microcontroller.

The fabrication of the probe was very challenging due to the scale. The multimode fiber that was purchased was cut to length and fit into a 3D-printed holder that was attached directly to the spinning servo motor. The team intended to direct the light outward with a mirror, however, the team was ultimately unsuccessful. Instead, the light was obstructed in specific directions to facilitate the demonstration of the probe's rotation. See Appendix E for a detailed fabrication process.

Final Prototype

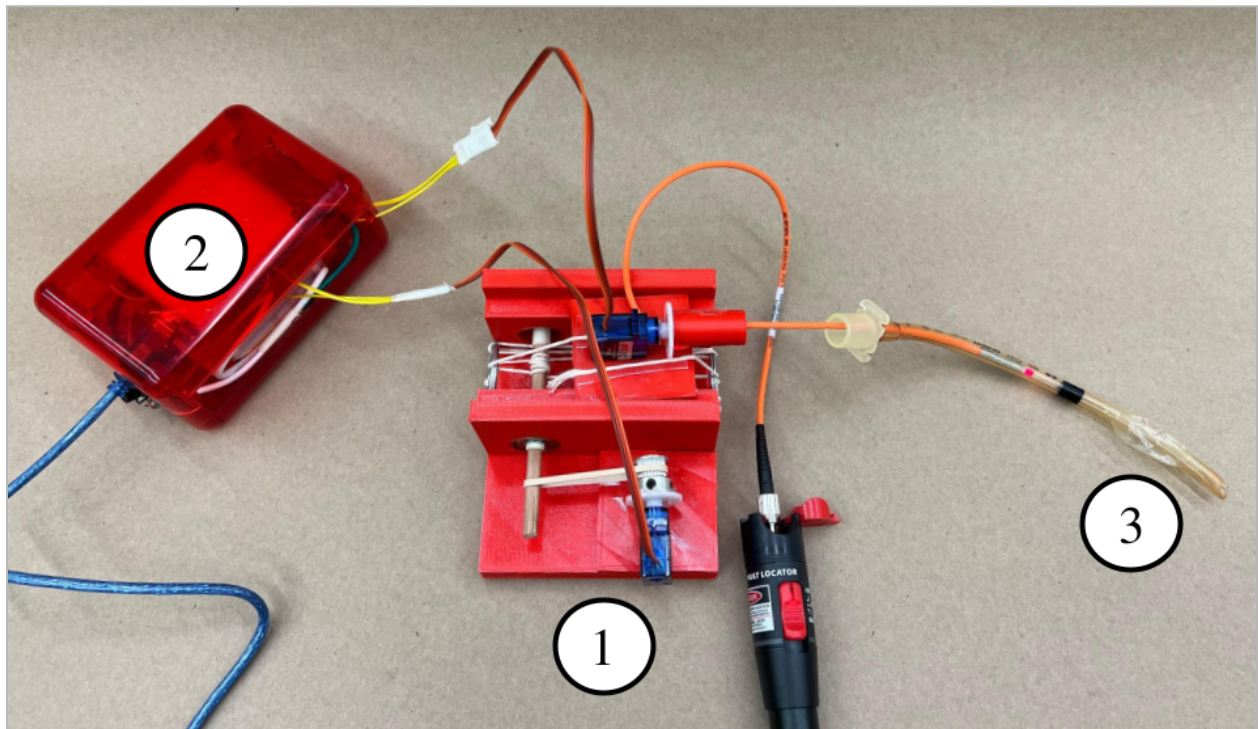


Figure 10: Full prototype broken down into three main sections: 1) Spinning Mechanism 2) Circuitry 3) Optical Probe

1) Spinning Mechanism

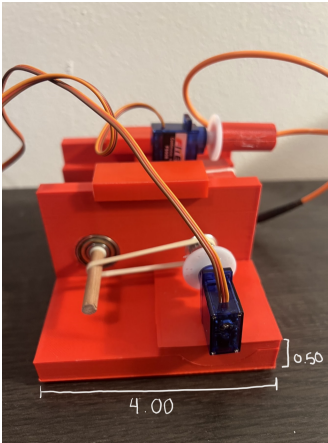


Figure 11: Front View
*Dimensions in inches

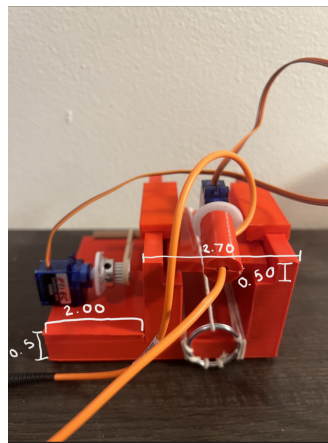


Figure 12: Right View

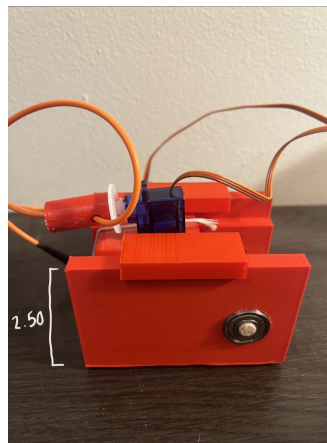


Figure 13: Back View

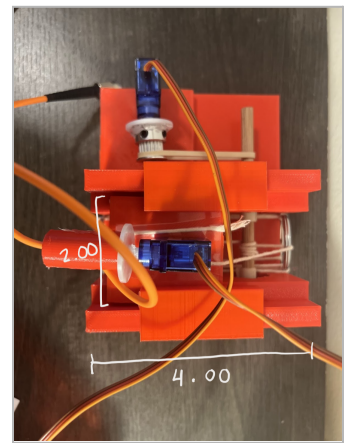


Figure 14: Top View

2) Circuitry

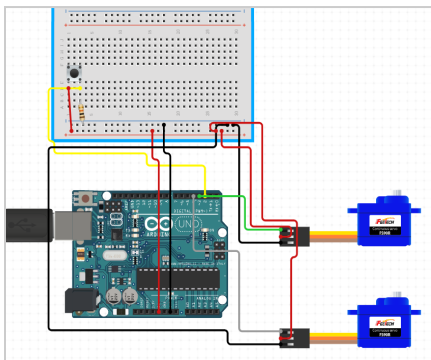


Figure 15: Digital Drawing of circuitry system

3) Optical Probe

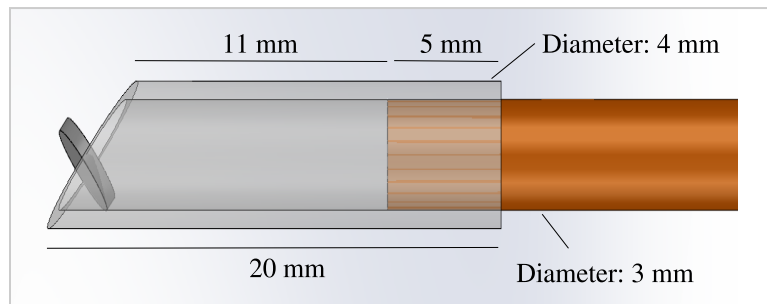


Figure 16: 3D drawing of optical probe

Testing

Testing of the device was split into three main components: measuring the retraction depth consistency, ensuring the optical fiber would spin 360°, and ensuring the light would appear horizontally to properly image the mouse airway.

Retraction depth consistency testing was done using a standard set up and measuring the distance the optical fiber was retracted for every slice. This consisted of securing the catheter and placing the optical fiber tip at a marked location to start every trial. The optical fiber was then retracted four times, measuring the distance from the marked start after each retraction. The distance traveled for each retraction was then calculated using the change in distance from the marked position after each retraction. This procedure was repeated for a total of 10 trials. This test was intended to measure the operational consistency of the optical fiber retraction both within one trial and over many separate trials. Intended results of the test would include a consistent retraction depth among all measurements taken. Consistent retraction depth will be measured based on if there is a statistically significant difference in retraction depth of a given slice. Notably, this would suggest that measurements will have a consistent total distance and the image slice distribution would be uniform.

Both 360° rotation and 90° light appearance were assessed during the testing of the retraction depth consistency. Full optical fiber rotation was assessed by placing the light source in the vertical position (0°) and observing it during testing to ensure it would rotate completely and return at least as far as the vertical position. Intended results of this test would be for the optical fiber to fully rotate everytime signaling the design is effective allowing for the acquisition of a complete radial image. Horizontal light appearance was measured during the retraction testing. Measurement consisted of noting the direction of the visible light coming from the optical fiber as either horizontal, coming out of the optical fiber perpendicular to the fiber direction, or vertical, coming out of the optical fiber parallel to the fiber direction. This was noted for all testing trials. Intended results of this test would be horizontal light appearance for every trial, signifying the capacity to image the airway mucosa.

VI. Results

Results for the retraction depth test showed there was consistency with clicks 2, 3, and 4. With click 1 the optical fiber occasionally hit the platform during rotation which caused the platform to jump and may have led to the 1st click average retraction distance being significantly higher ($p=0.032$, $n=40$) than the retraction distance of the other three clicks. The optical fiber never hit the platform on click 2, 3, or 4 which led to no significant differences in the average retraction distance as observed in Figure 6. To mediate this problem the team added rails on top of the base to keep the platform in place. The average total distance retracted was 2.5 cm which is longer than an average mouse endotracheal tube length of slightly under 2 cm with bodyweight greater than 17g [12]. The graph is labeled as slices to represent the distance that an image slice would be captured. The outcome of the rotation test was 360° rotation in all test cases. The outcome of the light test was light was shined horizontally, perpendicular to the

optical fiber, into the catheter 100% of the time with no escaped light. All of the test results support that the prototype will achieve this semester's goal for rotation and retraction of the optical fiber.

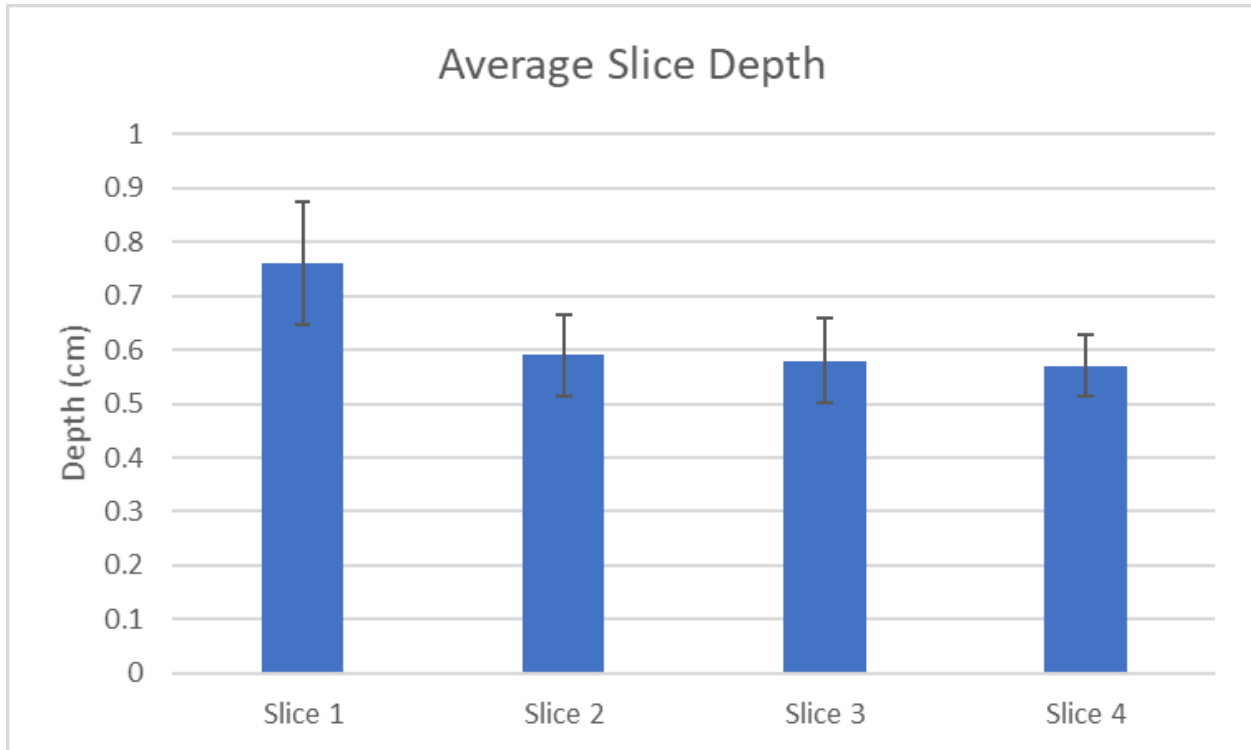


Figure 17: Graph showing average distance moved at each click in cm.

VII. Discussion

The intubation catheter must be minimally invasive in order to protect the test subjects and to ensure the highest accuracy in the images produced. If the catheter itself is contributing to the inflammation response in the mucosa then it will skew if not invalidate the results. Aspects like these will be assessed if Dr. Brasier takes a drug into clinical trials, therefore the final machine must limit physical contact as much as possible. There are also animal care standards and regulations relevant to the design, however, the restraints due to data accuracy require a much higher degree of animal protection than is required by regulation [9][11]. Material limitations include any material that is not biocompatible and would enter the mouse airway in any use case [9]. After testing how far the platform moved after the first click of the button, it was observed the platform jumped due to the optical fiber colliding with it. This jump could lead to an error in recording data or may cause the catheter to hit the mouse airway leading to potential damage. The team added guard rails to limit the platform from jumping but to prevent this entirely, the optical fiber would need to be positioned in a way that rotation does not lead to contact with the platform. Another potential source of error could be due to the leakage of current through the circuits. Since a minuscule amount of current is leaked through the circuitry,

it could cause errors in slightly over measuring the distance traveled by the platform or rotation of the optical fiber before the button is pressed. Lastly, the team attempted to reflect incoming light from the optical fiber onto a reflective surface, but was unable to form a high resolution reflection due to the form of light used. This was due to the need to cut the optical fiber lining and expose the inner fibers, preventing the light from being uniformly directed onto the reflective surface. To solve this issue, the team was able to manually direct the light by covering the end of the optical fiber to allow light to shine at a 90° angle.

VIII. Conclusions

Optical imaging tools are intricate and expensive machines that provide scientists and medical professionals an essential insight into biological organisms. The team developed a device that rotated and retracted an optical fiber by an electronic mechanism which can build a foundation for this project in future semesters. Specifically, the team's client, Dr. Brasier, intended to measure the inflammation of the airway mucosa in mice, an indicator of deteriorating health to assess the efficacy of novel drugs. For this task, optical coherence tomography (OCT) is well suited to produce high-resolution, volumetric images to completely image the mucosa. The team quickly learned from their professional advisors that to make a device like this would traditionally take a team of graduate students and much more than the budget for this semester. In spite of this, the team believes that over several courses of BME design, a completed OCT imaging device can be delivered to Dr. Brasier.

The team's final design consisted of a 3D printed base with holes and fittings to hold the axle and servo motors. One servo motor would contribute to the retraction aspect of the optical fiber within the catheter through a belt drive mechanism. The second servo motor would contribute to a complete 360° rotation of the optical fiber. This mechanism working together would allow for a wide range of imaging within the mucosa. The final product was not only able to retract and rotate the optical fiber but able to shine light through it that is directed out of the catheter. Unfortunately, the final design was too large to implement on mice and was unable to be attached to an imaging system to capture and process high resolution images. In the future, the team would like to see the intubation catheter scaled down to fit into a mouse airway as well as directing the reflected light into an imaging system. The team could further improve the prototype by using materials with a higher degree of safety and durability. Finally they would want to test the prototype with a mouse in vivo.

IX. References

- [1] J. B. Soriano, P. J. Kendrick, and K. R. Paulson, “Prevalence and attributable health burden of chronic respiratory diseases, 1990-2017: A systematic analysis for the global burden of disease study 2017,” *The Lancet. Respiratory medicine*, Jun-2020. [Online]. Available: <https://www.ncbi.nlm.nih.gov/pmc/articles/PMC7284317/>. [Accessed: 11-Oct-2022].
- [2] H. Wein, Ed., “Marvels of mucus and phlegm,” *National Institutes of Health*, 01-Sep-2020.[Online]. Available: <https://newsinhealth.nih.gov/2020/08/marvels-mucus-phlegm#:~:text=An%20infection%20can%20make%20mucus,arrive%20to%20fight%20the%20infection.> [Accessed: 12-Oct-2022].
- [3] B. J. Vakoc, M. Shishko, S. H. Yun, W.-Y. Oh, M. J. Suter, A. E. Desjardins, J. A. Evans, N. S. Nishioka, G. J. Tearney, and B. E. Bouma, “Comprehensive esophageal microscopy by using optical frequency–domain imaging (with video),” *Gastrointestinal Endoscopy*, 26-Mar-2007. [Online]. Available: <https://www.sciencedirect.com/science/article/pii/S0016510706026691>. [Accessed: 20-Sep-2022].
- [4] L. P. Hariri, M. B. Applegate, M. Mino-Kenudson, E. J. Mark, B. D. Medoff, A. D. Luster, B. E. Bouma, G. J. Tearney, and M. J. Suter, “Volumetric optical frequency domain imaging of pulmonary pathology with precise correlation to histopathology,” *Chest*, Jan-2013. [Online]. Available: <https://www.ncbi.nlm.nih.gov/pmc/articles/PMC3537541/>. [Accessed: 20-Sep-2022].
- [5] M. Eskandari, M. R. Pfaller, and E. Kuhl, “On the role of mechanics in chronic lung disease - researchgate,” *ResearchGate*, Nov-2013. [Online]. Available: https://www.researchgate.net/publication/261018942_On_the_Role_of_Mechanics_in_Chronic_Lung_Disease. [Accessed: 11-Oct-2022].
- [6] S. Aumann, S. Donner, J. Fischer, και F. Müller, ‘Optical Coherence Tomography (OCT): Principle and Technical Realization’, στο *High Resolution Imaging in Microscopy and Ophthalmology: New Frontiers in Biomedical Optics*, J. F. Bille, Επιμ. Cham: Springer International Publishing, 2019, σσ. 59–85.
- [7] C. G. Irvin and J. H. T. Bates, “Measuring the lung function in the mouse: The challenge of Size,” *Respiratory research*, 15-May-2003. [Online]. Available: <https://www.ncbi.nlm.nih.gov/pmc/articles/PMC184039/>. [Accessed: 22-Sep-2022].

- [8] Z. Yaqoob, J. Wu, και C. Yang, ‘Spectral domain optical coherence tomography: a better OCT imaging strategy’, *BioTechniques*, τ. 39, τχ. 6S, σσ. S6–S13, 2005.
- [9] “PHS Policy on Humane Care and Use of Laboratory Animals.” *National Institutes of Health*, U.S. Department of Health and Human Services, <https://olaw.nih.gov/policies-laws/phs-policy.htm#HealthResearchExtensionActof1985>.
- [10] Zare, Mina, et al. “Silicone-Based Biomaterials for Biomedical Applications:Antimicrobial Strategies and 3D Printing Technologies.” Wiley Online Library, *Journal of Applied Polymer Science*, 1 July 2021, <https://onlinelibrary.wiley.com/doi/full/10.1002/app.50969>. [Accessed: 11-Oct-2022]
- [11] “The Federal Register.” *Federal Register :: Request Access*, <https://www.ecfr.gov/current/title-9/chapter-I/subchapter-A/part-4>.
- [12] N. Nosaka , T. R. Crother, S. Chen, M. Arditi, and K. Shimada, “Optimal tube length of orotracheal intubation for mice,” *Laboratory animals*, 13-Apr-2018. [Online]. Available: <https://pubmed.ncbi.nlm.nih.gov/29649932/>. [Accessed: 11-Dec-2022].

X. Appendix

A: Product Design Specification

Function:

The goal of this project is to create and validate an optical frequency domain imaging (OFDI) probe for imaging in the airway of small animals. The cells lining the airway play an important role in common airway diseases and new therapeutics are being developed for treatment. A limitation in the work to develop these therapeutics is the difficulty of measuring changes over the course of an experiment. Some imaging techniques, including OFDI, are able to monitor changes in the airway; however, they are too large for small animal testing. Due to this problem, the aim of this project is to create an effective miniaturized OFDI probe for the use in animal testing.

Client requirements:

- The imaging device must be able to visualize the airway mucosa of mice in vivo.
- The device must be able to be maneuvered through a mouse airway for imaging.
- The project's budget is up to \$10,000 depending on availability of already purchased resources

Design requirements:

1. Physical and Operational Characteristics

a. Performance Requirements: The imaging device must be able to image the airway mucosa of a murine test subject. The device should be able to measure up to 1 mm in depth of the airway mucosa and should have a resolution of 5 - 20 μm , which is comparable to existing OCT systems [1]. The device should not harm the mouse when sedated to allow for testing throughout a drug testing protocol.

b. Safety: The device must come with clear and concise instructions for device usage and must only be used by a trained operator with animal subjects training [2]. The device material must not cause biological harm to the mouse or the user and no sharp edges should be exposed as part of the device that could cause internal injury to the mouse subject during imaging.

c. Accuracy and Reliability: The device must have a Signal to Noise Ratio (SNR) of 80 or more, which is a baseline for imaging biological targets [3]. The imaging

device must also demonstrate significant correlation ($p < 0.01$) between calculated airway wall layer areas using histology, ex-vivo, and in-vivo approaches [4].

d. Life in Service: The imaging probe should be reusable on different subjects, operating at least 10 minutes per use, averaging 2 minutes per data set with OFDI technology, [5] or 4 minutes with OCT technology [6]. The material of the probe will be sterilized by autoclaving.

e. Shelf Life: The shelf life will be dependent on quality of materials, e.g. fiber optic cable, biocompatible finish.

f. Operating Environment: The imaging probe must withstand temperatures between 20°C (68 °F) and 135°C (275 °F) for storage and sterilization conditions. The probe must also avoid corrosion from in-vivo testing and sterilization chemicals.

g. Ergonomics: The imaging probe must be made out of a material that can be used safely inside an organism with no reaction and can be sterilized. It must be able to maneuver the cartilage rings in the upper part of the trachea and measure within the airway mucosa [7].

h. Size: The probe must be able to fit inside the airway of a mouse. Its diameter must be less than 1.5mm, the diameter of a mouse trachea [8].

i. Weight: The probe must be light enough to be hand maneuvered by the same hand and weigh no more than 5.1 pounds [9].

j. Materials: Potential materials that may be included are fiber-optic cables, silicone rubber, and a camera and lens. The materials will all be biocompatible and autoclavable if the design is made to be reusable.

k. Aesthetics, Appearance, and Finish: The finish must be smooth to limit physical interference of the sample. The finish must be biocompatible. The appearance and aesthetic of the device does not contribute meaningfully to its efficacy .

2. Production Characteristics:

a. Quantity: The team will manufacture one final design and test it in the small

airway mucosa of a small mouse.

b. Target Product Cost: The manufacturing cost may be more expensive due to the specialized style of optical imaging necessary. The total cost should be approximately \$5,000-\$10,000. Although this cost is high, the total cost can be made lower based on materials already readily available to the team.

3. Miscellaneous

a. Standards and Specifications: Must avoid or minimize discomfort, distress or pain consistent with sound scientific practices [10]. Animals that are subject to prolonged discomfort or distress must be given proper sedation [10]. Animals must be humanely and safely be handled, treated and transported [11].

b. Customer: The customer is asking for a device which can image the mucosa in lab mice to record the effects of trial drugs. Mice are sedated prior to imaging. Perturbation of the mucosa and other tissue by the probe would negatively impact the accuracy of the data taken. The customer would like a feature of the probe to indicate the depth of the probe in the mouse.

c. Subject-related concerns: The materials and maneuverability of the probe must ensure the mouse is unharmed and procedures follow lab animal safety protocol while using the product.

d. Competition: Hariri et. al. published a study in 2012 recording the use of OFDI on human lung imaging. The study described two methods, one of bronchoscopy airway-centered imaging and one of parenchymal imaging. A custom-built bronchoscope was used with a diameter of 0.8 - 1.7 mm. The OFDI methods were only performed on human lungs [12].

Templin et. al. published a study in 2010 that successfully used OFDI for stent healing evaluation in vevo on pigs. The study described using a Terumo-OFDI catheter on a 0.014-inch guidewire. The study successfully used OFDI on the animals 1, 3, 10, 14, and 28 days after the stents were implanted [13].

Vakoc et. al. published a study in 2006 where OFDI was successfully performed on the distal esophagus of two swine using a 4.5 cm long inflatable balloon. The study successfully acquired cross sectional imaging of the mucosal vascular network within two living swine [14].

No patents were found for a product that could successfully use OFDI in the airways of any animals smaller than pigs.

PDS References:

- [1] S. Aumann, S. Donner, J. Fischer, και F. Müller, ‘Optical Coherence Tomography (OCT): Principle and Technical Realization’, στο High Resolution Imaging in Microscopy and Ophthalmology: New Frontiers in Biomedical Optics, J. F. Bille, Επιμ. Cham: *Springer International Publishing*, 2019, σσ. 59–85.
- [2] *What Investigators Need to Know Who Must Comply With the PHS Policy?*, vol. NIH Publication No. 16-OD-6009. 2016.
- [3] Z. Yaqoob, J. Wu, και C. Yang, ‘Spectral domain optical coherence tomography: a better OCT imaging strategy’, *BioTechniques*, τ. 39, τχ. 6S, σσ. S6–S13, 2005.
- [4] J. N. S. d’Hooghe, A. W. M. Goorsenberg, D. M. de Bruin, J. J. T. H. Roelofs, J. T. Annema, και P. I. Bonta, ‘Optical coherence tomography for identification and quantification of human airway wall layers’, *PLoS One*, τ. 12, τχ. 10, σ. e0184145, Οκτωβρίου 2017.
- [5] M. J. Suter, B. J. Vakoc, P. S. Yachimski, M. Shishkov, G. Y. Lauwers, M. Mino-Kenudson, B. E. Bouma, N. S. Nishioka, and G. J. Tearney, “Comprehensive microscopy of the esophagus in human patients with optical frequency domain imaging,” *Gastrointestinal Endoscopy*, 26-Sep-2008. [Online]. Available: <https://www.sciencedirect.com/science/article/pii/S0016510708018361>. [Accessed: 22-Sep-2022].
- [6] V. Kaul, “Optical coherence tomography for Barrett esophagus,” *Gastroenterology & hepatology*, Apr-2018. [Online]. Available: <https://www.ncbi.nlm.nih.gov/pmc/articles/PMC6009188/>. [Accessed: 22-Sep-2022].
- [7] C. G. Irvin and J. H. T. Bates, “Measuring the lung function in the mouse: The challenge of Size,” *Respiratory research*, 15-May-2003. [Online]. Available: <https://www.ncbi.nlm.nih.gov/pmc/articles/PMC184039/>. [Accessed: 22-Sep-2022].
- [8] K. Kishimoto and M. Morimoto, “Mammalian tracheal development and reconstruction: Insights from in vivo and in vitro studies,” *Development (Cambridge, England)*, 01-Jul-2021. [Online]. Available: <https://www.ncbi.nlm.nih.gov/pmc/articles/PMC8276987/#:~:text=The%20diameter%20of%20the%20mouse,different%20between%20mice%20and%20humans.> [Accessed: 22-Sep-2022].
- [9] C. Zingale, V. Ahlstrom, and B. Kudrick, “Human Factors Guidance for the Use of

- Handheld, Portable, and Wearable Computing Devices ,” *FAA human factors (ang-E25) 2005-human factors guidance for the use of handheld computing devices*, Nov-2005. [Online]. Available: <https://hf.tc.faa.gov/publications/2005-human-factors-guidance-for-the-use-of-handheld/>. [Accessed: 22-Sep-2022].
- [10] “PHS Policy on Humane Care and Use of Laboratory Animals.” *National Institutes of Health*, U.S. Department of Health and Human Services, <https://olaw.nih.gov/policies-laws/phs-policy.htm#HealthResearchExtensionActof1985>.
- [11] “The Federal Register.” *Federal Register :: Request Access*, <https://www.ecfr.gov/current/title-9/chapter-I/subchapter-A/part-4>.
- [12] L. P. Hariri, M. B. Applegate, M. Mino-Kenudson, E. J. Mark, B. D. Medoff, A. D. Luster, B. E. Bouma, G. J. Tearney, and M. J. Suter, “Volumetric optical frequency domain imaging of pulmonary pathology with precise correlation to histopathology,” *Chest*, Jan-2013. [Online]. Available: <https://www.ncbi.nlm.nih.gov/pmc/articles/PMC3537541/>. [Accessed: 20-Sep-2022].
- [13] C. Templin, M. Meyer, M. F. Müller, V. Djonov, R. Hlushchuk, I. Dimova, S. Flueckiger, P. Kronen, M. Sidler, K. Klein, F. Nicholls, J.-R. Ghadri, K. Weber, D. Paunovic, R. Corti, S. P. Hoerstrup, T. F. Lüscher, and U. Landmesser, “Coronary optical frequency domain imaging (OFDI) for in vivo evaluation of Stent Healing: Comparison with light and electron microscopy,” *European heart journal*, Jul-2010. [Online]. Available: <https://www.ncbi.nlm.nih.gov/pmc/articles/PMC2903715/>. [Accessed: 20-Sep-2022].
- [14] B. J. Vakoc, M. Shishko, S. H. Yun, W.-Y. Oh, M. J. Suter, A. E. Desjardins, J. A. Evans, N. S. Nishioka, G. J. Tearney, and B. E. Bouma, “Comprehensive esophageal microscopy by using optical frequency–domain imaging (with video),” *Gastrointestinal Endoscopy*, 26-Mar-2007. [Online]. Available: <https://www.sciencedirect.com/science/article/pii/S0016510706026691>. [Accessed: 20-Sep-2022].

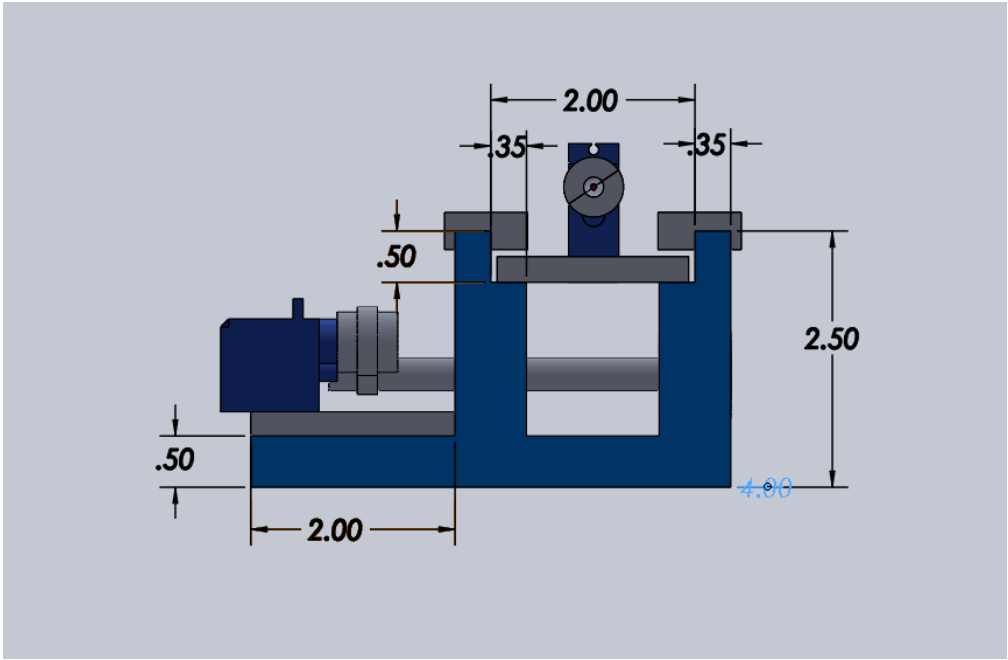
B: Testing Data

	Retracted Distance										
Trial	1 click	2 click	3 click	4 click	360 spin?	Light?					
1	0.7	1.4	2	2.5	yes	perpendicular	0.7	0.7	0.6	0.5	
2	0.5	1.5	2	2.4	yes	perpendicular	0.5	1	0.5	0.4	
3	1.4	2.2	2.6	2.9	yes	perpendicular	1.4	0.8	0.4	0.3	
4	0.5	1.2	2.1	2.7	yes	perpendicular	0.5	0.7	0.9	0.6	
5	1.3	2	2.4	2.9	yes	perpendicular	1.3	0.7	0.4	0.5	
6	0.4	0.6	1	1.9	yes	perpendicular	0.4	0.2	0.4	0.9	
7	0.4	0.7	1.4	2.2	yes	perpendicular	0.4	0.3	0.7	0.8	
8	0.6	1.2	2.2	2.8	yes	perpendicular	0.6	0.6	1	0.6	
9	0.9	1.4	2.1	2.7	yes	perpendicular	0.9	0.5	0.7	0.6	
10	0.9	1.3	1.5	2	yes	perpendicular	0.9	0.4	0.2	0.5	
avg	0.76	1.35	1.93	2.5		Avg each	0.76	0.59	0.58	0.57	0.625
	0.36	0.49	0.49	0.37			0.36	0.24	0.25	0.18	

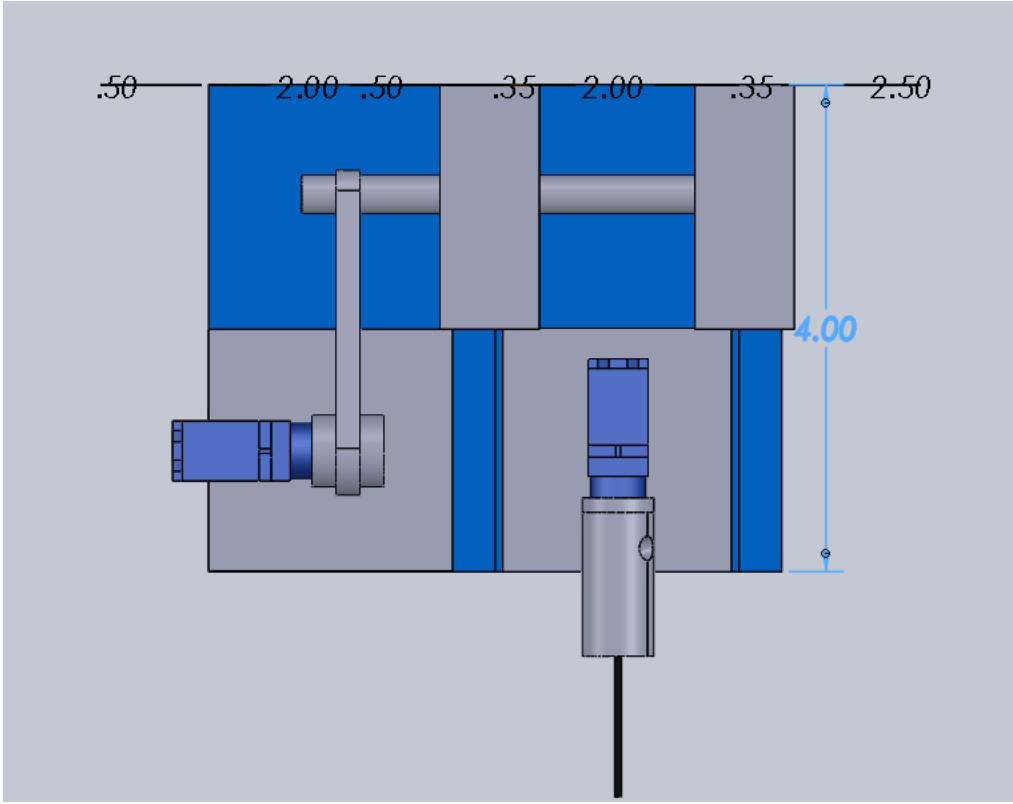
C: Team Expenses

Item	Description	Manufacturer	Part Number	Date	QTY	Cost Each	Total	Link
Optic Fiber Patch Cable	50 µm, 0.22 NA, FC/PC-FC/PC Fiber Patch Cable, 1 Meter	ThorLabs	M42L01	11/23	1	\$79.63	\$95.58	https://www.thorlabs.com/thorproduct.cfm?partnumber=M42L01
Optic Fiber Laser	HPOYUELC, 30km VFL Optical Fiber Cable Fault Tester, Optical Fiber Red Light Source Transmitter, Suitable for FC SC ST 2.5mm Universal Optical Fiber Connector.	HPOYUELC	B09XL2ND4J	11/23	1	\$16.89	\$17.55	https://www.amazon.com/HPOYUELC-Transmitter-Suitable-Universal-Connector/dp/B09XL2ND4J/ref=sr_1_5?crd=3DT1TDRG12J26&keywords=hpoyuclc+visual+fault+locator+30mw&qid=1670016338&prefix=visual+fault+locator+30mw%2C+HP%2Caps%2C68&sr=8-5
Arduino	Arduino UNO REV3	Arduino	A000066	11/23	1	\$23.46	\$24.18	https://www.amazon.com/Arduino-A000066-ARDUINO-UNO-R3/dp/B008GRSV6/ref=sr_1_3?crd=31PKEABX2J047&keywords=arduino+uno+a000066&qid=1670007399&prefix=arduino+uno+a000066%2Caps%2C66&sr=8-3
Motor	Greartisan DC 12V 100RPM Gear Motor High Torque Electric Micro Speed Reduction Geared Motor Centric Output Shaft 37mm Diameter Gearbox	Greartisan	B072R57C56	11/23	1	\$14.99	\$15.71	https://www.amazon.com/Greartisan-Electric-Reduction-Centric-Diameter/dp/B072R57C56/ref=sr_1_1?crd=11VNNZ2FMLZJV&keywords=greartisan%2Bdc%2B12v%2B100%2Brpm%2Bgear%2Bmotor%2Bhigh%2Btorque%2Belectric%2Bmicro%2Bspeed%2Breduction%2Bgeared%2Bmotor%2Bcentric%2Boutput%2Bshaft%2B37%2Bmm%2Bdiameter%2Bgearbo%2Caps%2C65&sr=8-1&th=1
Servo Motor	Feetech FS90R 360 Degree Continuous Rotation Micro Servo Motor + RC Tire Wheel for Arduino Microbit (Pack of 2)	DIYmalls	B079MF1BZS	11/23	1	\$14.98	\$15.64	https://www.amazon.com/Feetech-Degree-Continuous-Rotation-Arduino/dp/B079MF1BZS/ref=sr_1_1?crd=1142JNFKU1RDW&keywords=feetech+FS90R+360+degree+continuous+rotation+micro+servo+motor+%2B+RC+tire+wheel&qid=1670016553&prefix=feetech+fs90r+360+degree+continuous+rotation+micro+servo+motor+%2B+rc+tire+wheel%2Caps%2C64&sr=8-1
Relay Shield	HiLetgo 5V 4 Channel Relay Shield for UNO R3 Relay Shield Four Channel Relay Shield for UNO R3	HiLetgo	8541582938	11/23	1	\$7.99	\$8.65	https://www.amazon.com/HiLetgo-Relay-Shield-Channel-Arduino/dp/B07F7Y55Z7/ref=sr_1_1?crd=3RMO7876YZHSJ&keywords=Hiletgo+5v+4+channel+relay+shield+for+uno+r3&qid=1670016713&prefix=hiletgo+5v+4+channel+relay+shield+for+uno+r3+relay+shield+four+channel+relay+shield+for+uno+r3%2Caps%2C67&sr=8-1
Batteries	Energizer 2pk Max Alkaline 9V Batteries	Energizer	8080959	12/03	1	\$9.39	\$9.91	https://www.target.com/p/energizer-2pk-max-alkaline-9v-batteries/-/A-13738744#ink=sametab
Bearings	608 ZZ Ball Bearings, Skate Bearings Double Shielded Miniature Ball Bearings for Skateboards, Inline Skates, Scooters ABEC 7 Bearing (8mm x 22mm x 7mm) 4PCS	Homepal	B092LGTD9P	11/23	1	\$4.99	\$5.71	https://www.amazon.com/Bearings-Shielded-Miniature-Skateboards-Scooters/dp/B092LGTD9P/ref=sr_1_3?crd=3TPUFQXKZ6VFF&keywords=608+zz+ball+bearings%2C+skate+bearings+double+shielded+miniature+ball+bearings+for+skateboards%2C+inline+skates%2C+scooters+ABEC+7+bearing+%288mmx22mmx7mm%29+4+pack&qid=1670015769&prefix=608+zz+ball+bearings%2C+skate+bearings+double+shielded+miniature+ball+bearings+for+skateboards%2C+inline+skates%2C+scooters+abec+7+bearing+8mmx22mmx7mm+4+pack%2Caps%2C66&sr=8-3
3D Printed Base Pieces	NA	Makerspace	NA	12/05	24 hrs	\$14.08	\$14.08	NA
Total:						\$207.10		

D. Computer Aided Design Models (all dimensions in inches)



Front View of Mechanism Assembly with Dimensions



Top View of Mechanism Assembly with Dimensions

E. Fabrication Protocol

A. Spinning Mechanism

1. Servo motors, bearings, and the axle are measured precisely in order to be incorporated into the CAD design.
2. In Solidworks, the base and retractable platform are modeled to include fittings for all non-printed, moving parts.
3. Base and platform files are 3D printed using PLA plastic.
4. During assembly, a string is wrapped around the center of the axle, each end attaching to opposite sides of the retractable platform.
5. Servo motors are placed in dedicated fitments.
6. The belt drive from the axle to the servo conducting retraction is added.

B. Electronics

1. With the structure finished, the servo motors must be connected to power via the microcontroller.
2. Each servo's 3 pins are connected to 5V, GND, and a digital pin onboard the Arduino.
3. A switch button was connected to GND and to 5V via another digital Arduino pin.
4. With the button defined as an input and each servo defined as an output, a simple program was written that incrementally retracts the platform and performs 2 360° spins in opposite directions to return to the initial position. See Appendix F below for detailed code.

C. Optics

1. A 3D-printed fiber holder was modeled using the dimensions of the optic fiber.
2. Cut multimode optic fiber to allow light to exit the probe end.
3. Enclose the fiber in the 3D-printed housing.
4. Attach the base of the fiber holder to the servo on the retractable platform.
5. To demonstrate the rotation of the fiber in the catheter, obstruct a portion of the light leaving one side (along the axis) of the fiber to get an asymmetric beam.

F. Arduino Code

```
const int buttonPin = 2;
int buttonState = 0;
int pos = 0;
#define relay_4 4
#define relay_2 6

void setup() {
  Serial.begin(9600);
  myservo.attach(9);
  rotoservo.attach(4);
  pinMode(buttonPin, INPUT);
  myservo.write(90); // servo is stationary
  rotoservo.write(90); // servo is stationary
  Serial.println("reading");
  pinMode(relay_4, OUTPUT);
  pinMode(relay_2, OUTPUT);
  digitalWrite(relay_4, LOW);
  digitalWrite(relay_2, LOW);
}

void loop() {
  // put your main code here, to run repeatedly:
  buttonState = digitalRead(buttonPin);
  Serial.println(buttonState);

  if (buttonState == 1) {
    rotoservo.write(75); // start track servo
    delay(500);
    rotoservo.write(90);
    Serial.println("entered loop");
    int counter = 0;
    while (counter < 1) {
      myservo.write(110); // reverse
      delay(1250);
```

```

myservo.write(90); // stationary
delay(100); // delay .1 second

myservo.write(70); // forward
delay(1300); // delay 1 second

myservo.write(90); // stop

counter++;
}

// for (pos = 0; pos <= 180; pos += 1) { // goes from 0 degrees to 180 degrees
// // in steps of 1 degree
// myservo.write(pos); // tell servo to go to position in variable 'pos'
// delay(30); // waits 15 ms for the servo to reach the position
// Serial.println("finished first for loop");
// }
// for (pos = 180; pos >= 0; pos -= 1) { // goes from 180 degrees to 0 degrees
// myservo.write(pos); // tell servo to go to position in variable 'pos'
// delay(30);
// Serial.println("Finished second for loop.");
// }
}

Serial.println(buttonState);

}

```